DOI: 10.1002/adma.200700430

A Novel Method of Synthesis of Dense Arrays of Aligned Single Crystalline Copper Nanotubes Using Electrodeposition in the Presence of a Rotating Electric Field**

By *M. Venkata Kamalakar** and *Arup K. Raychaudhuri*

The discovery of carbon nanotubes[1] in 1991 initiated the interest on tubular nanostructures because of their immense fundamental importance as well as their potential applications in the nanoscale devices, sensors, catalysis, thermal materials, structural composites, field emission, biomedicine and energy storage/conversion.[2–7] Porous membranes such as anodic alumina, polycarbonate membranes, block copolymers etc. have opened up the possibilities of the synthesis of arrays of ordered nanowires of a number of materials. Use of electrodeposition to synthesize ordered arrays of nanowires in such templates is well studied.

However till date there are very few reports of the synthesis of arrays of metal nanotubes[8–15] using nanoporous templates. Most of the earlier work in this area involve chemical modification of the pore surface of porous templates to enhance the deposition of the metal on the pore walls. Such chemical modifications often add impurities to the nanotubes.[12,13] These methods are often specific for a particular kind of metal to be deposited and cannot be used for a variety of materials. Often it is also specific to an application. The processes are time consuming because of the complexities involved.[12,13] Thus a general and efficient method for the synthesis of metal nanotubes (with controlled length, diameter and wall thickness) still remains a challenge particularly in templates which allow synthesis of large ordered arrays.

We present here a novel, versatile and general approach for preparing metal nanotube (MNT) arrays. The method uses a template like anodic alumina and has full control on length, diameter and wall thickness of the nanotube. The method is general enough and in principle, can be applied to prepare single metal nanotubes of all metals which can be deposited by electrodeposition technique. This method in principle can also be used to deposit nanotubes of many semiconductors which can be prepared by electrodeposition.

The method of synthesis of metal nanotube arrays described here exploits the basic principle of electrodeposition in a rotating electric field, which we believe has never been utilized in such synthesis using electrodeposition. The novelty of this method lies in its generality, simplicity and efficiency. As a generic example, we report the synthesis of single crystalline copper nanotube arrays by electrodepositing copper into the pores of porous anodic alumina template in the presence of a lateral rotating electric field which is applied in addition to the longitudinal d.c electrodeposition current. The applied rotating field as our simulation shows (described later on) makes the ions graze the surface of the pores in helical paths and thus makes the deposition selectively occuring in the region near the wall of the nanopores.

The single crystalline copper nanotube arrays are prepared by electrodeposition in nanoporous anodic alumina membranes placed in the plane of a rotating electric field. Two sinusoidal electric fields of the same amplitude with a phase difference of $\pi/2$ (as shown in Scheme 1a) constitute the rotating electric field. The principle is well illustrated in Scheme 1. With average direct current densities (Faradic current that does the actual deposition) of 6 mA cm^{-2}, the time of deposition of the tubes in 200 nm pore diameter anodic alumina membranes (membrane area = 1 cm^2, membrane thickness = 60 μm) is 15–20 min. This shows that the method is relatively faster than other reported methods.[12,13]

This method gives very high quality MNT arrays as established by various structural characterization tools. Figure 1c shows a typical array of copper nanotubes fabricated by the method described, as imaged by a Scanning Electron Microscope (SEM). Figure 1d shows a closer view of the tubes protruding out from the partially etched anodic alumina template. The tubes shown in Figure 1, were fabricated in porous alumina templates with pore diameters specified as 200 nm. The wall thickness of these tubes as observed (upon further zooming into the image) is ~ 20 nm. The Energy-dispersive spectrometry (EDS) of the tips of the tubes revealed that these tubes are composed of the element copper.

The Transmission Electron Microscope (TEM) image (Fig. 2a) shows clearly that these tubular structures have constant wall thickness throughout their length. Figure 2b shows a 160 nm diameter tube with a thickness of approximately 15 nm. The selective area diffraction pattern of a single nano-

[*] M. V. Kamalakar, Prof. A. K. Raychaudhuri
DST Unit for Nanosciences, Department of Materials Science
S N Bose National Centre for Basic Sciences
Block-JD, Sector-III, Salt Lake, Kolkata 700 098 (India)
E-mail: venkat@bose.res.in

[**] The authors thank the Department of Science and Technology, Govt. of India for financial support in the form of a Unit. MVK thanks CSIR, Govt. of India for fellowship. We also thank the Unit for Nanoscience and Technology, Indian Association for the Cultivation of Science, Kolkata, India for TEM support. Surface physics division, SINP, Kolkata is highly acknowledged for SEM support.

ADVANCED MATERIALS

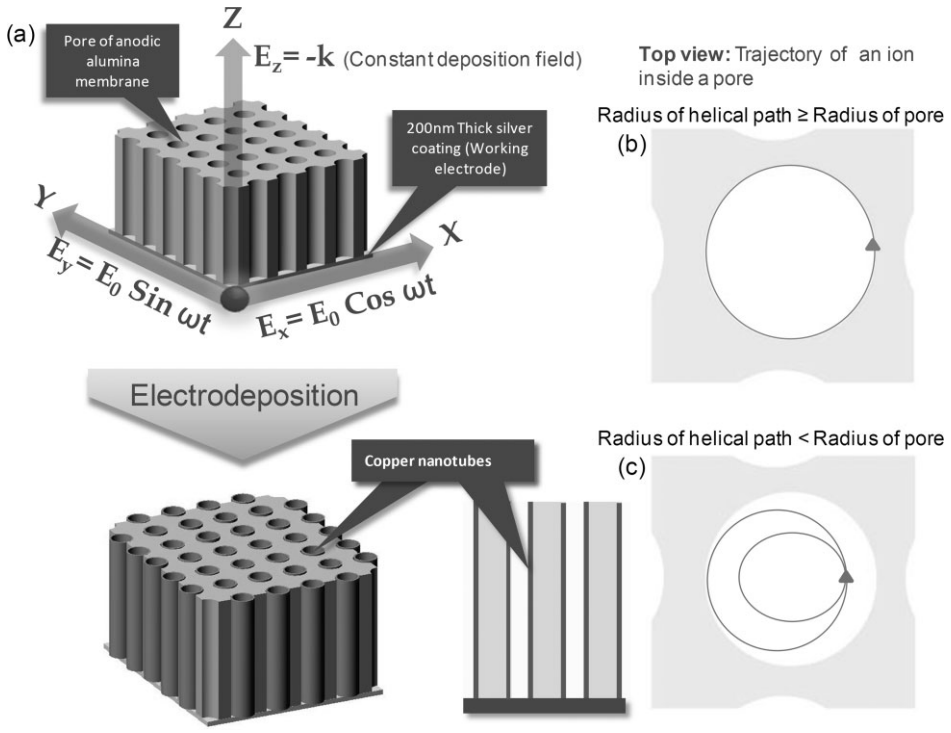

Scheme 1. a) Detailed principle of synthesis of metal nanotubes. b) The trajectory of an ion with the radius of its helix ≥ pore radius. c) The trajectory of an ion with the radius of its helix < pore radius.

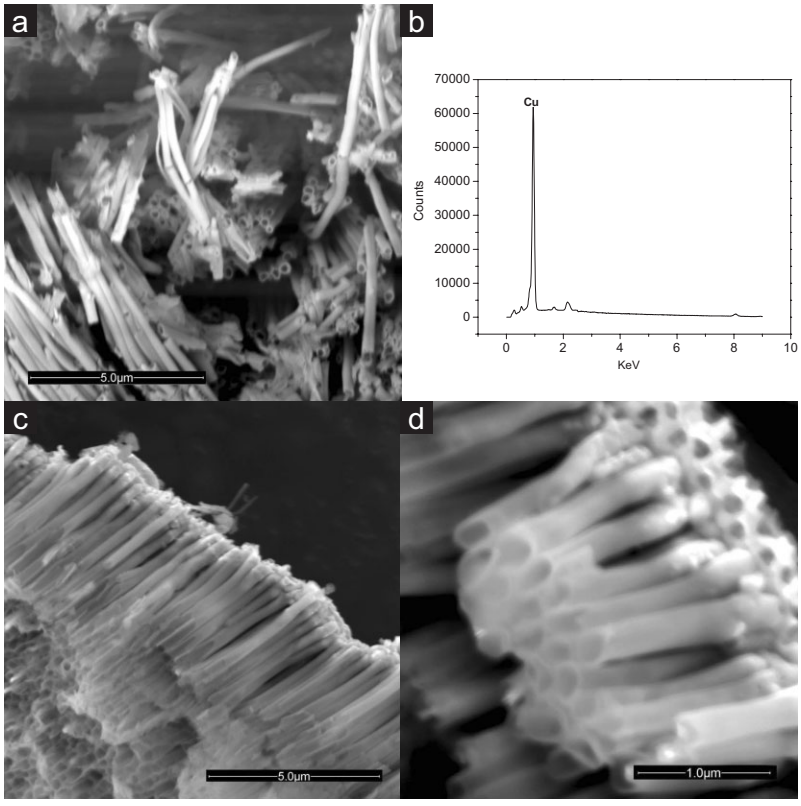

Figure 1. a) Copper nanotubes after the removal of alumina templates. b) EDS Spectrum of the copper nanotubes. c) SEM image of a large array of copper nanotubes. d) Side view of the nanotubes (The wall thickness is clearly visible).

tube is shown in Figure 2c. The diffraction data is indexed into the (220) plane. The TEM data shows that these tubes are single crystalline in nature. The single-crystalline nature of the MNT arrays have been further established by X-Ray diffraction (XRD). A typical XRD pattern of the as synthesized samples is shown in Figure 2d. The XRD data were taken by retaining the MNTs within the template. The reflections are indexed to the face-centered cubic (fcc) structure (Space group: Fm3m). No other peaks were obtained except those of copper which indicates the purity of the nanotubes formed. The XRD pattern (Fig. 2d) shows that the (220) reflection is the only prominent peak in comparison to the other reflections, indicating the fact that the array of tubes have a preferential growth direction along the (220) plane. The XRD data are in conformity with the TEM diffraction data presented before.

The electrodeposition technique that is widely used to make metal nanowires in templates uses the deposition field which is essentially longitudinal so that they are along the axis of the pore. Our innovation is based on controlling the motion of ions during electrodeposition and restricting the ions to the walls of the pores. This is achieved by a rotating electric field which is always perpendicular to the electrodeposition field and thus the extra field forces the ions to graze along the surface of the walls. The rotating electric field is produced by perpendicular superposition of two sinusoidal electric fields (of identical amplitude and frequency) to each other, differing by a phase of $\pi/2$. This is in accordance with the Lissajous figures where two sinusoidal signals with identical amplitude and frequency give rise to a circle when superposed perpendicularly with a phase difference of $\pi/2$. Since the pores to be filled have circular cross section, we used a phase difference of $\pi/2$ between the lateral two sinusoidal fields. The electric fields acting on the ions are shown in Scheme 1.

The mechanism of the formation of nanotubes can be understood in the following way. Taking μ, the mobility of ions, the velocity V of

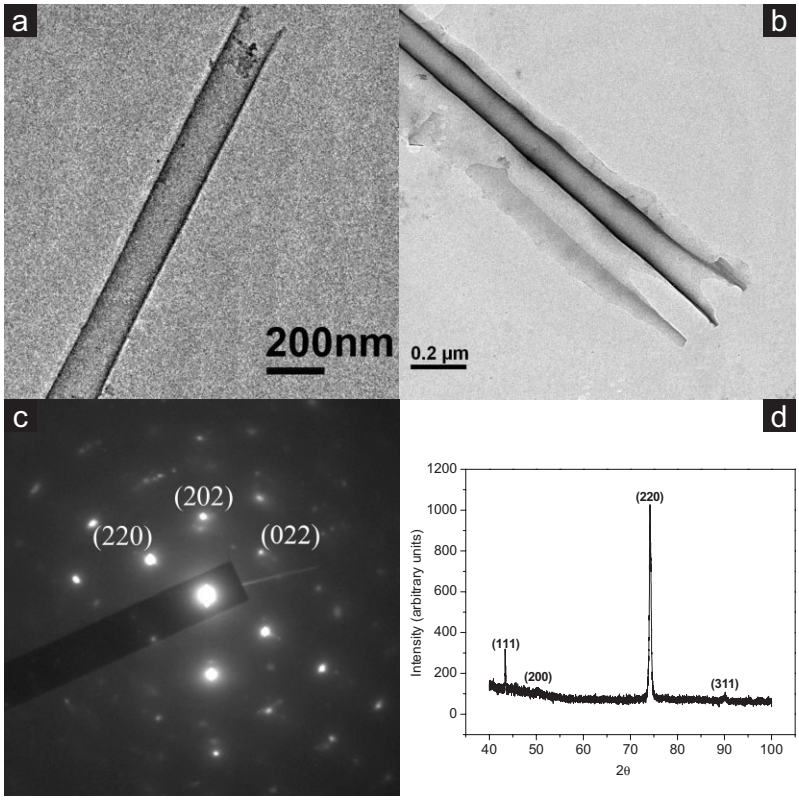

Figure 2. a) and b) TEM images of copper nanotubes after being separated from the alumina template. The tube in b) is partially broken to show the wall of the tube. c) Electron diffraction pattern of a tube. d) XRD pattern of the copper nanotubes.

an ion in an electric field E is proportional to the velocity, with μ, being the proportionality constant[16]

$$\vec{V} = \mu \vec{E} \tag{1}$$

We first consider the effect of the rotating field. With two sinusoidal electric fields acting along the x-axis and y-axis respectively, the two velocity components are

$$V_x = \frac{dx}{dt} = \mu E_0 \cos \omega t \tag{2}$$

and

$$V_y = \frac{dy}{dt} = \mu E_0 \sin \omega t \tag{3}$$

These equations essentially imply

$$X = \frac{\mu E_0}{\omega} \sin \omega t \tag{4}$$

and

$$Y = -\frac{\mu E_0}{\omega} \cos \omega t \tag{5}$$

So the motion of the ion due to the superposition of the electric fields follows a circular orbit with a radius R

$$R = \frac{\mu E_0}{\omega} \tag{6}$$

When the process of electrodeposition is started, an additional electric field E_z acts along the z-axis making the trajectory of each ion a helix. The radius of such a helix is given by R which can easily be tailored by the field amplitude E_0 and frequency ω. Thus each ion gets deposited following such a trajectory. Within the pores of the template the motion of the ions gets constrained by the pore walls if the radius R is more than or equal to the pore radius R_0. This way ions, irrespective of their initial positions, upon reaching the pore walls will move staying close to the surface wall of the pores. For a given pore radius R_0 we can define a critical field $E_c = \frac{\omega R_0}{\mu}$ where $R = R_0$. When $E_0 \geq E_c$ the depostion will occur preferentially at the pore wall.

The above simple picture of the formation of nanotube with a rotating field of constant amplitude (E_0) at all points along the radius of the tube, however, gets modified in the real situation. The field seen by the ions is not the same as the applied electric field because of the much larger dielectric constant of the electrolyte compared to the surrounding alumina. If E_0 is the amplitude of the applied field, the amplitude of the field deep inside the electrolyte is $\mathrm{E_{Elec}} = \mathrm{E_0} \frac{2K_{\mathrm{Alumina}}}{K_{\mathrm{Alumina}} + K_{\mathrm{Elec}}}$, where K denotes the dielectric constant of the medium concerned. However, this field reduction will not occur abruptly at the alumina – electrolyte interface. The applied electric field decays exponentially to E_{elec} with a characteristic Debye screening length[17] $\lambda = \sqrt{\frac{\varepsilon_r \varepsilon_0 kT}{e^2 C_0}}$, where ε_0 is the permittivity of free space, ε_r is the dielectric constant, k is the Boltzmann's constant, T is the temperature, e is the elementary charge, and C_0 is the ionic concentration. Using the relevant numbers we find that the screening length λ is comparable to the radius of the pore and thus the field is not screened abruptly at the interface. This makes the electric field dependent on the distance from the tube wall and thus a function of the position. As a result one cannot use the simple relation as given in Equation 6 to find the radius of the tube formed.

To test the above mechanism of formation of the nanotubes, we made a computer simulation of the experiment using the above model and the field amplitude profile given by the relation $\mathrm{E(r)} = \mathrm{E_{Elec}} + (\mathrm{E_0} - \mathrm{E_{Elec}})\mathrm{e}^{-\frac{(\mathrm{R_0}-\mathrm{r})}{\lambda}}$ instead of simply E_0. r is the distance from the centre along the radius and λ is the characteristic screening length.

The results from the simulation show that the thickness of the nanotube $\Delta R/R_0$ (expressed as fraction of pore radius R_0)

ADVANCED MATERIALS

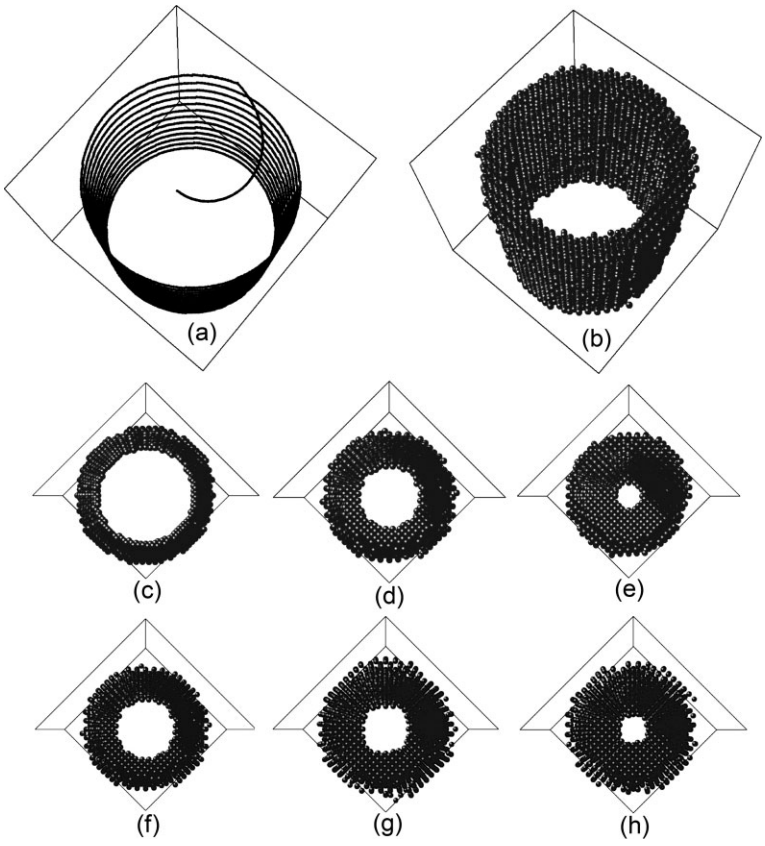

Scheme 2. a) Typical trajectory of an ion. b) Nanotube formed by electrodepositing 50000 atoms in a pore having 10 nm diameter. Frequency of the rotating electric field is 20 Hz. c)–e) correspond to the tubes formed for descending lateral field amplitudes $1.13E_c$, E_c, $0.86E_c$ for the same $\lambda/R_0 = 0.47$. f)–h) Represent the tubes formed for 0.47, 0.4, 0.33 of λ/R_0, respectively at $E_0 = E_C$.

has a simple dependence on the parameter λ/R_0 for a given applied field and as one would expect $\Delta R/R_0$ increases as λ/R_0 becomes smaller. For a given λ/R_0 the wall thickness $\Delta R/R_0$ also depends on E_0. Our computer simulations reveal that for $\lambda R_0 \geq 0.47$, with $E_0 \geq E_C$, any ion, irrespective of its initial position, manages to reach the pore walls and traverses a helix grazing the surface of the pore (Scheme 1b) before getting deposited when it comes in contact with the atoms of the working electrode or the growing deposition front. A typical trajectory of a single ion for such a case is shown in Scheme 2a. For other values of λ/R_0 and E_0 (unless E_0 is too high such that $E_{Elec} \sim E_C$), the trajectory becomes helical with fluctuating radii (Scheme 1c). Formation of a nanotube with diameter ~ 10 nm, with 50000 atoms (whose initial positions and velocities are randomized) is shown in Scheme 2b. The nanotube so formed in the simulation has a wall thickness ~ 2 nm. This is a typical example of a metal nanotube formation.

In the Scheme 2c–e we show development of tubes of different thicknesses for the same $\lambda_0/R_0 = 0.47$ but for different E_0. Our simulations also reveal that for $E_0 = E_C$, the tube formation initiated even with values starting from $\lambda/R_0 \sim 0.2$ and for fields $E_0 > E_C$, tube formation can occur even with $\lambda/R_0 \leq$ 0.2. For a fixed field ($E_0 = E_C$) the development of tubes for different λ/R_0 is shown in Scheme 2f–h.

The frequency of rotating electric field determines the number of revolutions an ion makes grazing the wall surface of the pore before getting deposited. This is very important in the formation of a tube with uniform wall thickness. In our experiment, for the actual growth we chose a frequency of around 10 Hz in such a way that the ions make enough revolutions along the pore walls through a column of 60 μm pore depth before getting deposited. The lateral rotating electric field is produced by two pairs of copper plates, each pair being perpendicular to the other. Each pair consists of two rectangular shaped copper electrodes kept parallel to each other separated by a distance of 2 cm. With these specifications and taking the standard mobility of copper ions[16] as 5.56×10^{-8} m^2 s^{-1} V^{-1} we chose the voltage amplitude (V_0) of the rotating electric field ($E_0 = V_0/d$; d being the distance between the electrode pairs) as 3 V ($E_0 > E_C$ corresponding to 100 nm) to get a helical path of ion perfectly grazing the wall of a pore of radius 100 nm.

From the simulation results, we infer that for a radius of 100 nm, a screening length $\lambda \geq 20$ nm will result in the formation of a tube at $E_0 = E_C$. For $E_0 > E_C$, the tube formation can take place even with $\lambda < 20$ nm. This is the typical value of the screening length for electrolytes with ionic concentrations closer to millimoles. Due to the depletion of ions due to deposition and inhomogeneity (refer to experimental), the electrolyte inside pores is of approximately millimolar concentration and this initiates the formation of the tubular structures.

Figure 3a shows the result of electrodeposition in the porous membrane in the absence of a lateral electric field. In the absence of a rotating field one obtains nanowires, as expected. The effect of the lateral rotating electric field of 3 V (voltage amplitude) is shown in Figure 3b, which shows a large array of MNT with wall thickness ~ 15–20 nm. A decrease in the lateral electric field is seen to increase the wall thickness, as evident from Figure 3e ($V_0 = 2$ V) and Figure 3f ($V_o = 1.5$ V). This will correspond to the tube formation for the simulation shown in Scheme 2e ($E < E_c$). The resulting tubes have wall thicknesses of 70 nm and 95 nm respectively with outer tube diameters being 230 nm. From the simulation we expect the wall thickness to be ≈ 85 nm and 110 nm, respectively for $V_0 = 2$ V and 1.5 V. Thus our simulation results agree reasonably well with the experimental results. This establishes the fact that the basic mechanism proposed for the formation of the tube is correct. The thickness of deposition also depends on the time of deposition. After the initiation of the tube wall growth, the modified electrodeposition field lines which will mostly terminate on the top edge of the tube wall periphery, will favor the growth of the tube further. The exact formula-

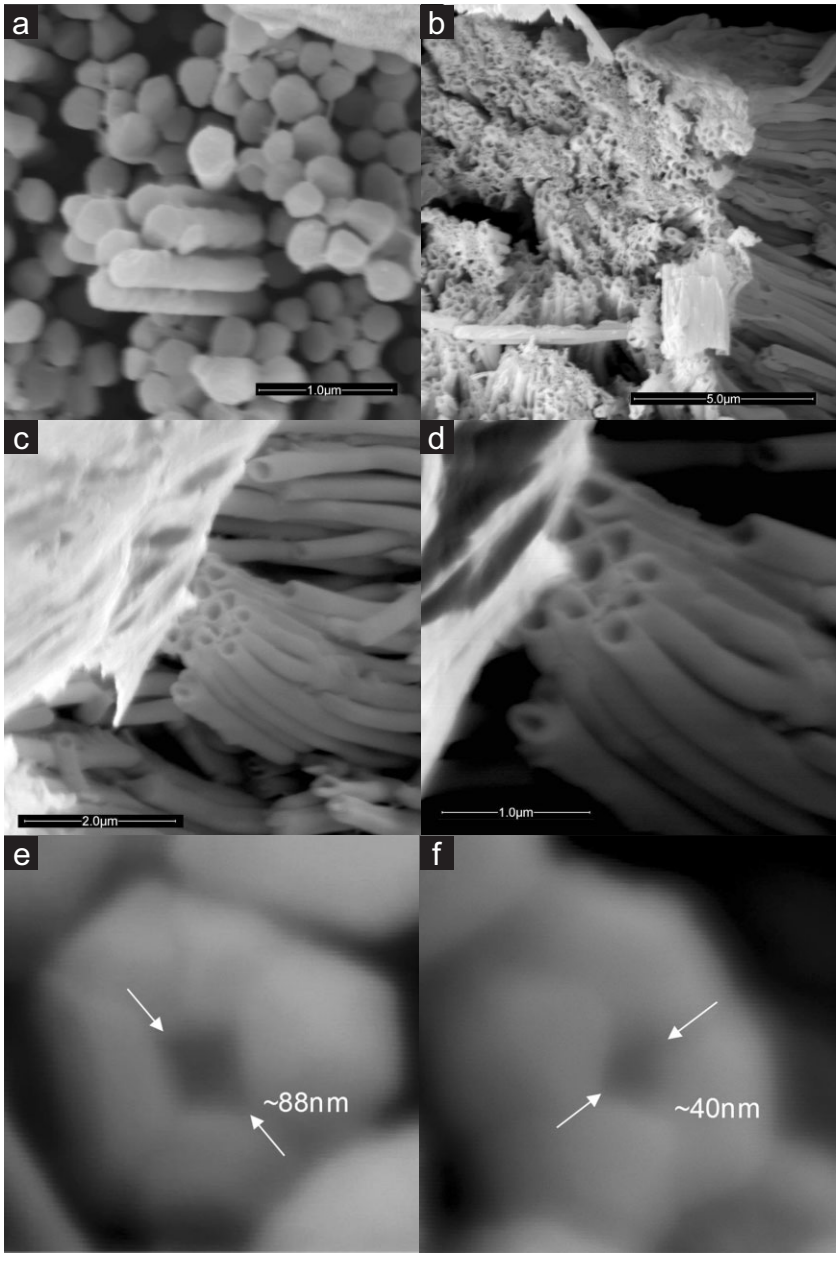

Figure 3. a) SEM image of Copper nanowires formed with the voltage amplitude of lateral rotating electric field zero. b) A large array of copper nanotubes formed with the voltage amplitude 3 V. c) Side view of the copper nanotubes (Voltage amplitude 3 V). d) Closer view of copper nanotubes (Voltage amplitude 3 V). e) SEM images of single copper nanotube of 230 nm diameter (Voltage amplitude 2 V). f) SEM images of single copper nanotube having 230 nm diameter (Voltage amplitude 1.5 V).

tion of the tube thickness on the time and modified field lines are issues being considered for further study.

The principal benefit of this approach is that it is general, and it does not need any chemical modification or partial coating of the pores for synthesizing the nanotubes. The method also does not alter the chemistry of the standard electrodeposition that is used for a given material. It only changes the external electric field configuration. Thus this can be applied to the synthesis of any metal/compound nanotubes which can be electrodeposited. The simulation of the method gives a physical insight into how metal nanotubes can be formed inside porous templates. To our knowledge this is the first method which is not only simple and fast but also based on designing the shape of an electrodeposited metal by controlling the ionic dynamics inside an electrolyte. The MNT have a constant wall thickness throughout the length as seen in the TEM images. Thus they can act as a hollow nanoelectrode and give options of filling them with other materials like semiconductors and high dielectric constant materials for such applications in fields like nanoelectronics, solar cells, supercapacitors etc.

An important issue in formation of metallic nanotubes is its chemical purity in addition to its structural integrity. To test that we measured the resistance of the nanotubes from 4.2 K to 300 K. Electrical measurement of the nanotube arrays has been done by a pseudo four probe method[18] (refer Experimental Sec.). The resistance data is shown in Figure 4. The electrical resistance increases as a function of temperature, typical of metallic behavior, with residual resistivity ratio ($R_{300K}/R_{4.2K}$) of 3.5. This residual resistivity ratio is typical of copper films and is indicative of a reasonable chemical purity and absence of significant structural defects. The metallic behavior makes these single crystalline copper nanotubes highly promising materials for nanoelectronic applications.

In summary, ordered arrays of single crystalline copper nanotubes have been prepared by a novel potentiostatic electrodeposition technique in nanoporous templates in the presence of a lateral rotating electric field. The wall thickness of the metal nanotubes so obtained are in the range of 15–20 nm and can be controlled by changing the amplitude of the rotating field. The X-ray diffraction results show that the copper nanotubes grown have a preferential direction of growth. The electron diffraction results show that the tubes are single crystalline in nature. The study of electrical resistance as a function of temperature shows that these tubes have a metallic behavior. The synthesis method is a simple innovation that controls the ion dynamics during electrodeposition. We believe that this is a general method for growth of other metal nanotube arrays and can be applied to many materials which can be grown by electrodeposition

ADVANCED MATERIALS

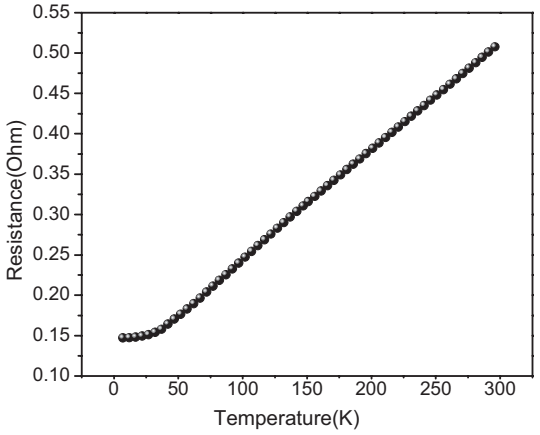

Figure 4. Electrical resistance as a function of temperature.

technique, including compound material nanotube arrays. We therefore expect that our method for the synthesis of metal nanotubes will lead to further development of a broad new class of materials for nanoelectronic devices. Further work is underway to formulate the details of the growth method and have better control on the thickness of the nanotube by understanding its dependence on the growth field.

Experimental

Anodic alumina and polycarbonate membranes (procured from Whatman Corp.) were used to prepare the copper nanotube arrays. The anodic alumina membranes specified as 200 nm are observed to have a pore size distribution varying from 150 nm to 300 nm with most of the pores having diameters ranging between 200–240 nm. A 200 nm thick layer of silver was sputtered on to one of the surfaces of the membrane. This silver layer acts as the working electrode in the three electrode potentiostatic electrodeposition. A Saturated Calomel Electrode (SCE) was used as the reference electrode. A platinum wire was used as the counter electrode. A 1 M $CuSO_4 \cdot 5H_2O$ (99.995 % purity, procured from Sigma–Aldrich) is slowly injected in the millipore water taken in the electrodeposition cell through a nozzle at the top of the cell during electrodeposition. The deposition is stopped when an abrupt rise in current is observed as indication of growth of tube over the complete lengths of the pores.

Electrodeposition was carried out at a potential of –0.3 Volt with respect to the SCE. The membrane was placed in the plane of a rotating electric field during electrodeposition. The lateral rotating electric field was created by two pairs of parallel copper electrodes perpendicular to each other and separated by Teflon spacers. If the two pairs of electrodes are placed along the *x* and *y* axis, then the deposition is carried out along the *z* axis with the template placed in the middle of the four electrodes making the sides of a square. A sinusoidally varying voltage from a signal generator was applied to one of the pair of parallel copper electrodes. A similar signal was phase shifted by $\pi/2$ and was applied to the other pair of copper electrodes. The frequency used in the experiment was 10 Hz.

For imaging by scanning electron microscope (SEM), the template containing the nanotubes is etched partially with 3 M NaOH solution to dissolve most of the aluminium oxide layer. The remaining template after washing several times with Millipore water was used for the imaging. SEM images were taken with the Quanta 200 FEG SEM (FEI Co.) For Transmission Electron Microscopy (TEM), the template was completely etched with 6M NaOH solution and washed 10 times with Millipore water before spraying on a carbon coated copper grid. Images were obtained by a JOEL, JEM-2010 having LaB_6 electron gun for operation between 80-200kV. Structural characterization was done by PANALYTICAL X-ray powder diffractometer with Cu Kα radiation (λ = 1.5418 Å) with the nanotubes remaining embedded in the template.

Electrical characterization has been done by measuring the resistance using a pseudo four probe method by retaining the nanotubes within the alumina template which being made of alumina is insulating. Two copper wire contacts are made on each side of the anodic alumina template using a conductive silver adhesive paste from Alfa Aeser. Each pair of copper wires served as current and voltage probes on each side of the template containing nanotubes. Electrical resistance as a function of temperature is measured in a pulse tube cryogenerator (CRYOMECH, Model PT405 Cryogenic Refrigerator).

Received: February 18, 2007
Revised: August 16, 2007
Published online: December 7, 2007

[1] S. Iijima, *Nature* **1991**, *354*, 56.
[2] J. Hu, T. W. Odom, C. M. Lieber, *Acc. Chem. Res.* **1999**, *32*, 435.
[3] R. Tenne, A. K. Zettl, *Top. Appl. Phys.* **2001**, *80*, 81.
[4] G. R. Patzke, F. Krumeich, R. Nesper, *Angew. Chem. Int. Ed.* **2002**, *41*, 2446.
[5] C. N. R. Rao, M. Nath, *Dalton Trans.* **2003**, 1.
[6] C. R. Martin, *Chem. Mater.* **1996**, *8*, 1739.
[7] S. B. Lee, D. T. Mitcell, L. Trofin, T. K. Nevanen, H. Soderlund, C. R. Martin, *Science* **2002**, *296*, 2198.
[8] a) C. R. Martin, *Science* **1994**, *266*, 1961. b) J. D. Klein, R. D. Herric, D. Palmer, M. J. Sailor, C. J. Brumlik, C. R. Martin, *Chem. Mater.* **1993**, *5*, 902.
[9] a) C. J. Brumlik, C. R. Martin, *J. Am. Chem. Soc.* **1991**, *113*, 3174. b) K. B. Jirage, J. C. Hulteen, C. R. Martin, *Science* **1997**, *278*, 655. c) M. Wirtz, S. F. Yu., C. R. Martin, *Analyst* **2002**, *127*, 871.
[10] J. C. Bao, C. Y. Tie, Z. Xu, Q. F. Zhou, D. Shen, Q. Ma, *Adv. Mater.* **2001**, *13*, 1631.
[11] a) B. Mayers, Y. N. Xia, *Adv. Mater.* **2002**, *14*, 279. b) B. Mayers, X. C. Jiang, D. Sunderland, B. Cattle, Y. N. Xia, *J. Am. Chem. Soc.* **2003**, *125*, 13364.
[12] C. Mu, Y. Yu, R. Wang, K. Wu, D. Xu, G. Guo, *Adv. Mater.* **2004**, *16*, 550.
[13] F. Tao, M. Guan, Y. Jiang, J. Zhu, Z. Xu, Z. Xue, *Adv. Mater.* **2006**, *18*, 2161.
[14] H. Cao, L. Wang, Y. Qui, Q. Wu, G. Wang, L. Zhang, X. Liu, *ChemPhysChem* **2006**, *7*, 1500.
[15] T. Sehayek, M. Lahav, R. Popovitz-Biro, A. Vaskevich, I. Rubinstein, *Chem. Mater.* **2005**, *17*, 3743.
[16] P. W. Atkins, *Physical Chemistry* (Ed: J. De Paula), Oxford University Press, Oxford **1998**.
[17] J. O'M. Bockris, A. K. N. Reddy, *Modern Electrochemistry, Ionics*, Vol. 1, Plenum, New York, pp. 230–248.
[18] A. Bid, A. Bora, A. K. Raychaudhuri, *Phys. Rev. B* **2006**, *74*, 035426.

